Heliyon 10 (2024) e32270

Contents lists available at ScienceDirect

Heliyon

journal homepage: www.cell.com/heliyon

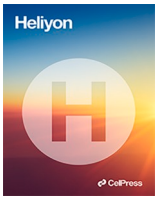

Research article

A cuproptosis-related gene DLAT as a novel prognostic marker and its relevance to immune infiltration in low-grade gliomas

Peng Gao [a,b,*,1], Huaixu Li [b,1], Yang Qiao [b], Jianyu Nie [b], Sheng Cheng [c], Guozhang Tang [d], Xingliang Dai [b,e], Hongwei Cheng [b]

[a] Department of Neurosurgery, Affiliated Jinling Hospital, Medical School of Nanjing University, Nanjing, 210002, PR China
[b] Department of Neurosurgery, The First Affiliated Hospital of Anhui Medical University, Hefei, 230022, PR China
[c] Department of Clinical Medicine, The First Clinical College of Anhui Medical University, Hefei, 230022, PR China
[d] Department of Clinical Medicine, The Second Clinical College of Anhui Medical University, Hefei, 230022, PR China
[e] Department of Research & Development, East China Institute of Digital Medical Engineering, Shangrao, 334000, PR China

ARTICLE INFO

Keywords:
Cuproptosis
DLAT
Biomarker
LGG
Immune infiltration

ABSTRACT

DLAT has been recognized as a cuproptosis-related gene that is crucial for cuproptosis in earlier research. The study is to look at how DLAT affects individuals with low-grade glioma's prognosis and immune infiltration. The Genotype-Tissue Expression (GTEx) database and the TCGA database were used in this work to download RNAseq data in TPM format. DLAT was found to be overexpressed in LGG by comparing DLAT expression levels between LGG and normal brain tissue, and the expression of DLAT was verified by immunohistochemistry and semi-quantitative analysis. Then, the functional enrichment analysis revealed that the biological functional pathways and possible signal transduction pathways involved were primarily focused on extracellular matrix organization, transmembrane transporter complex, ion channel complex, channel activity, neuroactive ligand-receptor interaction, complement and coagulation cascades, and channel activity. The level of immune cell infiltration by plasmacytoid dendritic cells and CD8 T cells was subsequently evaluated using single-sample gene set enrichment analysis, which showed that high DLAT expression was inversely connected with that level of infiltration. The link between the methylation and mRNA transcription of DLAT was then further investigated via the MethSurv database, and the results showed that DLAT's hypomethylation status was linked to a poor outcome. Finally, by evaluating the prognostic value of DLAT using the Cox regression analysis and Kaplan-Meier technique, a column line graph was created to forecast the overall survival (OS) rate at 1, 3, and 5 years after LGG identification. The aforementioned results demonstrated that high DLAT expression significantly decreased OS and DSS, and that overexpression of DLAT in LGG was significantly linked with WHO grade, IDH status, primary therapy outcome, overall survival (OS), disease-specific survival (DSS), and progression-free interval (PFI) events. DLAT was discovered as a separate predictive sign of OS in the end. DLAT might thus represent a brand-new predictive biomarker.

* Corresponding author. Department of Neurosurgery, the First Affiliated Hospital of Anhui Medical University, 218 Jixi Road, Hefei 230022, PR China.
E-mail address: gaopeng@ahmu.edu.cn (P. Gao).
[1] These authors contributed equally to this work.

https://doi.org/10.1016/j.heliyon.2024.e32270
Received 27 September 2023; Received in revised form 24 May 2024; Accepted 30 May 2024
Available online 6 June 2024

1. Introduction

Lung cancer, breast cancer, and brain tumors are the leading sources of high death rates, and both the growth and mortality rates of cancer have climbed substantially over the past few years [1,2]. Diffuse malignant glioma is an aggressive primary tumor of the central nervous system (CNS), accounting for about 81 % of all brain malignancies, and has a poor prognosis [3,4]. According to its pathological characteristics, gliomas were classed by the World Health Organization (WHO) as WHO 1–4 in 2021. Those with WHO 2/3 gliomas get a greater efficacy than those with WHO 4 gliomas, so the therapeutic value of LGG is relatively high [5]. Currently, the main treatment for LGG at WHO is still surgical resection and chemotherapy [6]. Yet, most patients miss the ideal window for surgical intervention because there aren't any overt clinical symptoms. Temozolomide has been demonstrated to increase the likelihood of developing acquired drug resistance when used as a first-line chemotherapy treatment [7]. As a result, the current overall survival rate for glioma patients remains low [8]. In summary, it is crucial to uncover potential prognostic biomarkers and treatment targets for LGG as well as to elucidate the molecular mechanisms underlying carcinogenesis.

The human body uses copper in a number of metabolic activities. A recent study by Tsvetkov and colleagues identified for the first time a different pathway of apoptosis than that associated with oxidative stress called cuproptosis [9]. During the onset of cuproptosis, The lipid acyl fraction serves as a direct copper-binding agent, which causes lipidated proteins to aggregate, proteins containing the Fe–S cluster to disappear, and the level of 70-kDa proteins involved in heat shock to increase, resulting in proteotoxic stress that directly affects the cellular TCA cycle and ultimately leads to cell death [9]. In order to cure disorders caused by genetic anomalies in copper homeostasis, Tang et al. demonstrated that copper chelators are essential [10]. The research revealed that ferricoxigenin 1, one of the cuproptosis-related genes, has a significant role in tumorigenesis (FDX1). Prior research has demonstrated that several cuproptosis-related genes are crucial in tumorigenesis, including ferricoxigenin 1 (FDX1) [11], dihydrolipoamide dehydrogenase (DLD) [12], and pyruvate dehydrogenase E1 subunit alpha 1 (PDHA1) [13]. According to the findings mentioned above, cuproptosis could serve as a target for cancer treatment. The Warburg effect, or aerobic glycolysis, is thought to be a sign of the spread and cancer progression [14]. It remains unclear, though, whether increased glycolysis is a contributing factor to or a result of the development of cancer [15]. The glycolytic molecule pyruvate can be transformed oxidatively to acetyl coenzyme A for the TCA cycle or reductively to lactate for glycolysis, both of which are mediated by the pyruvate dehydrogenase complex (PDC). Pyruvate dehydrogenase (E1), dihydrolipoyl transacetylase (E2, DLAT), dihydrolipoyl dehydrogenase (E3), and a structural subunit are the three catalytic subunits of human PDC (E3 binding protein) [16]. Previous studies have shown that DLAT catalyzes the breakdown of pyruvate to acetyl coenzyme A, and it facilitates the TCA cycle's metabolism by providing the TCA cycle's raw material [17]. These results imply that DLAT serves numerous roles in different malignancies. The tumorigenic function of DLAT in LGG, its clinical significance, and abnormalities in tumor immunological expression are presently unknown owing to the heterogeneity of LGG.

With the aid of bioinformatics, this investigation aims to explore and comprehend the connection among both DLAT expression and their clinicopathological and forecasting value, possible molecular mechanisms, and immunological cell infiltration. This understanding could aid clinicians in improving patient care and prognosis for those with low-grade gliomas.

2. Materials and methods

2.1. Brain tissue specimen

The glioma and paratumor specimens were acquired form the Department of Neurosurgery, the First Affiliated Hospital of Anhui Medical University. A total of 20 specimens from patients with gliomas were collected, including 10 pairs of grade I gliomas and 10 pairs of grade II. All specimens of glioma are confirmed to be primary tumors, without prior radiotherapy or chemotherapy before surgery. All glioma tissues were completely removed for the first time, and the prognosis was confirmed through postoperative pathological examination. Instantly following surgical resection, all specimens were instantly frozen in liquid nitrogen. All samples were taken and utilized after receiving the patient's informed consent and approval from the First Affiliated Hospital of Anhui Medical University's ethics committee (Ethics No. PJ2024-04-74).

2.2. Data gathering and analysis for RNA sequencing

RNAseq data in the TPM file for TCGA and GTEx handled consistently by the Toil method were obtained from UCSC XENA (https://xenabrowser.net/datapages) to examine DLAT expression in pan-cancer [18]. For the study of DLAT expression in tumor tissues, samples from the TCGA database [19] were chosen, and for the analysis of normal tissue samples, a combination of the TCGA and genotypic tissue expression (GTEx) datasets were used. The Human Protein Atlas (www.proteinatlas.org) contained immunohistochemical sections comparing low-grade glioma tumor tissue to normal brain tissue.

2.3. Brain histopathologic staining and immunohistochemistry (IHC)

Glioma specimens were made into 5-m-thick paraffin slices, and traditional paraffin-embedded sections were used for HE staining. Specimens were first soaked in xylene before being cleaned with alcohol (China Pharmaceutical Group Co., Ltd., Beijing, China). The sections were then sealed with serum and 3 % H_2O_2 after being decreased with 1 EDTA (Bixuan Biotechnology Co., Ltd., Shanghai, China). After incubated the slides with primary antibodies DLAT (DF14046) overnight at 4 °C. Then, secondary antibodies were incubated, followed by DAB (Baso Diagnostics Inc., Zhuhai, China) and hematoxylin staining. After that, neutral resin was used to seal

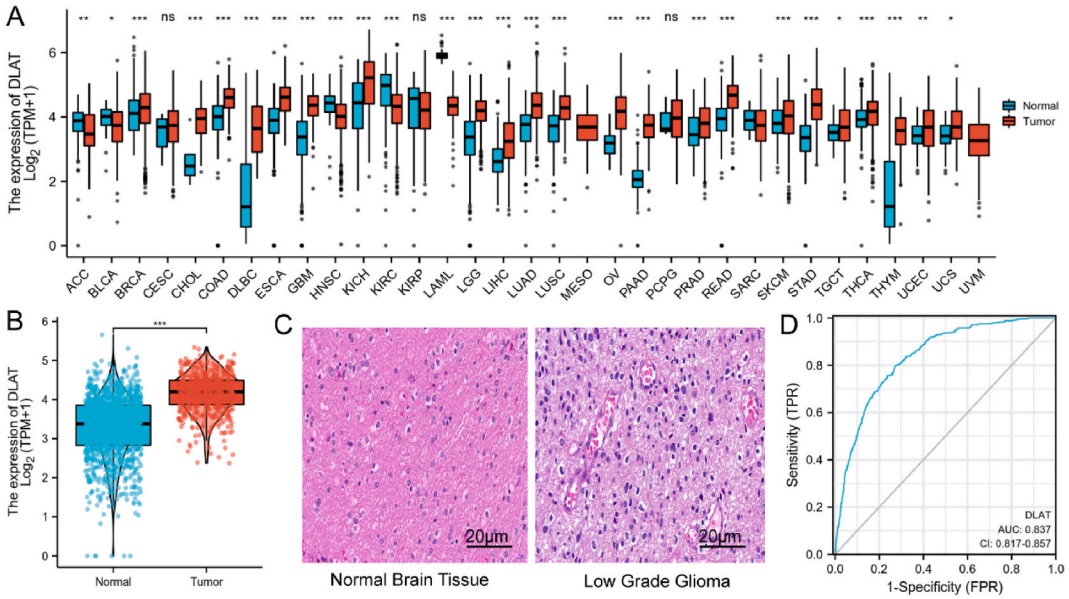

Fig. 1. Expression levels of DLAT in different types of tumors and low-grade gliomas. (A) Expression in different types of tumors compared to normal tissues in TCGA and GTEx databases, (B) expression in low-grade gliomas and non-matching normal tissues in TCGA and GTEx databases, (C) Histological staining of DLAT in normal brain t issue and glioma, (D) ROC curves used to classify DLAT versus normal brain tissues in TCGA database. ROC curves for classification. Scale bar = 20 μm * $p < 0.05$, ** $p < 0.01$, *** $p < 0.001$.

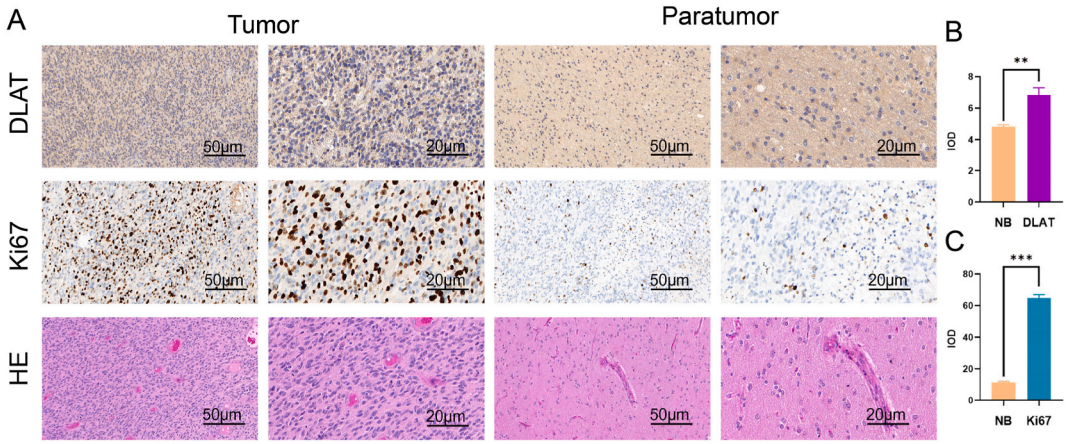

Fig. 2. Histological staining and immunohistochemistry and semi-quantitative analysis results of DLAT and Ki67 in paratumor and glioma. (A) Histological staining and immunohistochemistry of DLAT and Ki67 in paratumor and glioma; (B–C) Semi-quantitative analysis results of DLAT and Ki67. Scale bar = 20 μm. Scale bar = 50 μm ** $p < 0.01$, *** $p < 0.001$.

the slices (China Pharmaceutical Group Co., Ltd., Beijing, China). Proplus 6.0 software (Media Cybernetics, Inc., Rockville, MD, USA) and the value of integrated optical density (IOD) was assessed. Certain molecular markers abnormally expressed in glioma reported previously are assessed in this study, including VIM, IDH1, CD34, EMA, GFAP, P53, S100, and ATRX [20–23].

2.4. Analysis of differentially expressed genes

According to the mean DLAT expression value, patients with low-grade gliomas in the TCGA were divided into two groups: an elevated DLAT team and a decreased DLAT team. Differentially expressed gene (DEG) analysis was carried out among the two categories using the R program DESeq2, adjusted for p-value <0.05 [24], with |log2-fold-change (FC)|>1 designated to be the DEG criterion. Using Spearman's association analysis, the relationships among the top 10 DEGs and DLAT gene expression were evaluated.

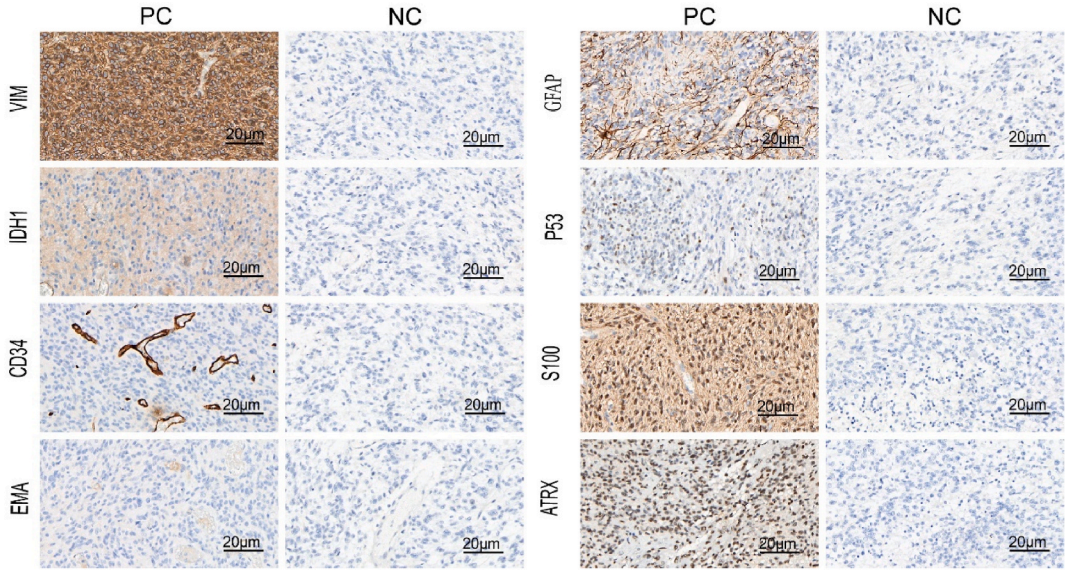

Fig. 3. Immunochemical staining of brain tissues. Including immunochemical staining of VIM, IDH1, CD34, EMA, GFAP, P53, S100, ATRX in glioma (Positive control PC, and Negative control NC). Scale bar = 20 μm.

2.5. Analysis of functional enrichment

R package GOplot (version 1.0.2) [25] was used to investigate DEG using functional enrichment analysis, which included Kyoto Encyclopedia of Genes and Genomes (KEGG) analysis and gene ontology (GO). The R package cluster profiler was used to perform gene set enrichment analysis (GSEA) [26]. Enrichment functions or pathways with adjusted p-values <0.05 and false discovery rates (FDR) < 0.25 were regarded as significant.

2.6. Immune infiltration analysis

Previous studies have shown that pDC and $CD8^+$ T cells play a critical role in the immunotherapy of cancer [27,28]. To thoroughly describe tumor-immune interactions in low-grade gliomas, a single-sample GSEA approach of the R new software GSVA (version 3.6) [29] was utilized. Utilizing gene expression profiling database, we investigated the connection among DLAT expression and inflammatory cells infiltration in the work. Wilcoxon rank sum and Spearman rank correlation tests were used to determine p-values in order to investigate the link between DLAT levels and the quantity of immune cells infiltrating malignancies.

2.7. Deoxyribonucleic acid methylation analysis

To investigate the potential mechanisms of DLAT on low-grade gliomas, an online program (MethSurv database [30]) was employed to evaluate the relationship among both the methylation levels and DLAT mRNA transcription based on multivariate survival analysis of DNA methylation data and the prognosis of DLAT methylation levels.

2.8. Survival analysis

The average DLAT's expression served as the threshold for the Kaplan-Meyer technique and log-rank test used in the survival analysis. Clinical factors' effects on patient outcomes were evaluated using univariate and multivariate Cox regression models. The multivariate Cox regression analysis used the prognostic variable $p < 0.1$ from the univariate Cox regression analysis. The ggplot2 R software was used to display forest maps.

2.9. Building and evaluating nomograms

In a multivariate Cox analysis, column line plots determined by specific prognostic variables were made to determine the overall survival chance. The outcomes of the column line plots were then evaluated using the calibration plots, as well as the discriminations of the column line plots were quantified using the consistency index. (C index). Through the R software, column line plots as well as calibration plots were produced. The temporal ROC software program was used to evaluate prediction accuracy using time-dependent subject operating characteristic (ROC) curves.

Table 1
Clinicopathological characteristics of DLAT low and high expression groups.

Characteristic	Low expression of DLAT	High expression of DLAT	p
n	255	255	
WHO grade, n (%)			<0.001
G2	123 (27.2 %)	93 (20.5 %)	
G3	92 (20.3 %)	145 (32 %)	
IDH status, n (%)			0.004
WT	34 (6.7 %)	60 (11.8 %)	
Mut	220 (43.4 %)	193 (38.1 %)	
1p/19q codeletion, n (%)			0.396
codel	79 (15.5 %)	89 (17.5 %)	
non-codel	176 (34.5 %)	166 (32.5 %)	
Primary therapy outcome, n (%)			<0.001
PD	36 (8.2 %)	65 (14.8 %)	
SD	62 (14.1 %)	81 (18.4 %)	
PR	38 (8.6 %)	24 (5.5 %)	
CR	78 (17.7 %)	56 (12.7 %)	
Gender, n (%)			0.656
Female	111 (21.8 %)	117 (22.9 %)	
Male	144 (28.2 %)	138 (27.1 %)	
Race, n (%)			0.477
Asian	3 (0.6 %)	5 (1 %)	
Black or African American	8 (1.6 %)	13 (2.6 %)	
White	237 (47.5 %)	233 (46.7 %)	
Age, n (%)			0.330
<=40	132 (25.9 %)	120 (23.5 %)	
>40	123 (24.1 %)	135 (26.5 %)	
Histological type, n (%)			0.155
Astrocytoma	97 (19 %)	95 (18.6 %)	
Oligoastrocytoma	72 (14.1 %)	56 (11 %)	
Oligodendroglioma	86 (16.9 %)	104 (20.4 %)	
Laterality, n (%)			0.582
Left	128 (25.3 %)	120 (23.8 %)	
Midline	2 (0.4 %)	4 (0.8 %)	
Right	123 (24.4 %)	128 (25.3 %)	
OS event, n (%)			0.002
Alive	208 (40.8 %)	177 (34.7 %)	
Dead	47 (9.2 %)	78 (15.3 %)	
DSS event, n (%)			0.014
Alive	208 (41.4 %)	181 (36.1 %)	
Dead	45 (9 %)	68 (13.5 %)	
PFI event, n (%)			0.055
Alive	170 (33.3 %)	148 (29 %)	
Dead	85 (16.7 %)	107 (21 %)	
Age, median (IQR)	39 (31, 52)	42 (33.5, 54)	0.046

2.10. Statistical analysis

R (version 3.6.3)9 was used to conduct all statistical studies. The Wilcoxon rank sum test along with the paired samples *t*-test was each used to determine the statistically significant level of DLAT expression in separated and matched tissues, respectively. The correlation among medical characteristics and DLAT overexpression was evaluated using the Wilcoxon rank sum test and the Logit model test. Each test had a two-sided p-value of 0.05 or below and was statically important [31,32].

3. Results

3.1. Elevated expression levels of DLAT in low-grade gliomas

DLAT expression in 33 tumors was analyzed using data downloaded from TCGA and GTEx. Fig. 1A demonstrates that DLAT was substantially expressed in the majority of malignancies, such as esophageal cancer (ESCA), diffuse large b-cell lymphoma (DLBC), cholangiocarcinoma (CHOL), and breast invasive carcinoma (BRCA). In Fig. 1B, compared to normal brain tissue, low-grade glioma samples showed considerably increased levels of DLAT expression ($p < 0.001$). Histological staining of DLAT in normal brain tissue and glioma (Fig. 1C). Also, the ROC curve in Fig. 1D demonstrated good discrimination between low-grade glioma tissues and normal tissues, with Shadows below the curve (AUC) of 0.837 (95 % confidence interval [CI] = 0.817–0.857).

In addition, the histopathologic morphology of glioma was found to be significantly different from that of its paraneoplastic tissue by HE staining. Immunohistochemical staining showed that glioma tissues were positive compared with the paracancerous tissues, indicating that DLAT is expected to be a novel prognostic marker for glioma (Fig. 2A). Immunohistochemical semi-quantitative

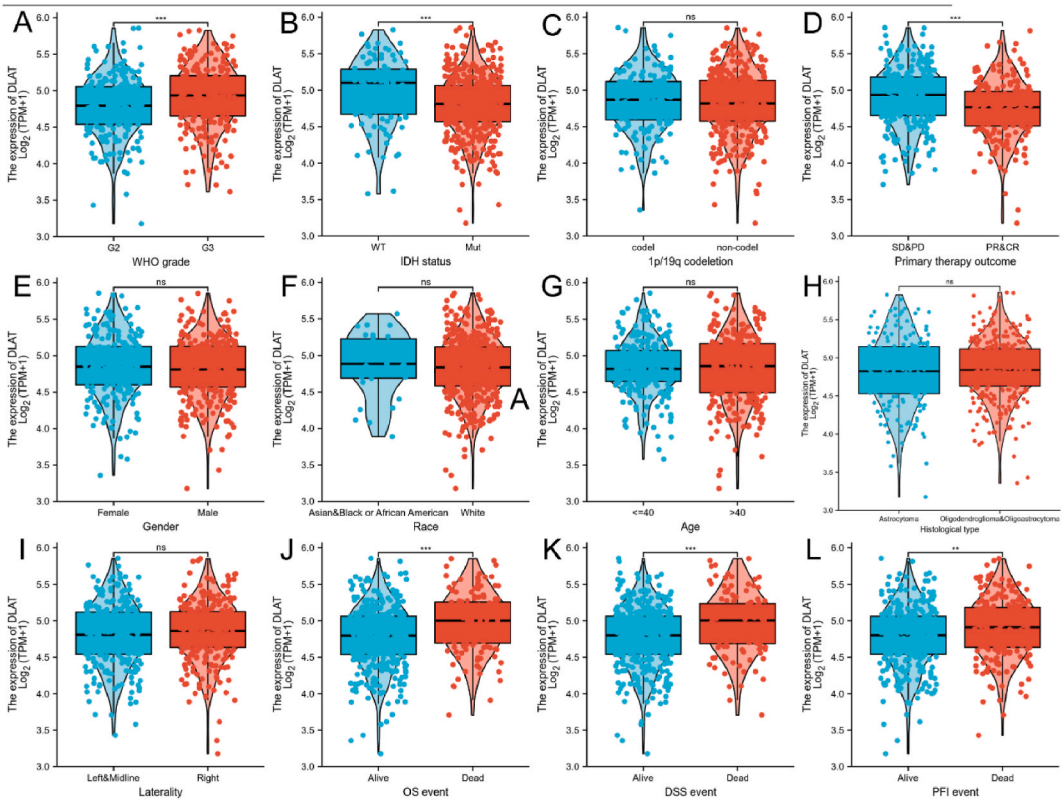

Fig. 4. Associations between DLAT expression and clinicopathological characteristics. Data are shown for (A) WHO grade; (B) IDH status; (C) 1p/19q codeletion; (D) Primary therapy outcome; (E) Gender; (F) Race; (G) Age; (H) Histological type; (I) Laterality; (J) OS event; (K) DSS event; (L) PFI event. *p < 0.05, **p < 0.01, ***p < 0.001.

Table 2
Association of DLAT expression with clinicopathological characteristics of patients.

Characteristics	Total(N)	Odds Ratio (OR)	P value
WHO grade (G3 vs. G2)	467	2.040 (1.413–2.957)	<0.001
1p/19q codeletion (non-codel vs. codel)	528	0.827 (0.573–1.190)	0.307
Primary therapy outcome (PR&CR vs. PD&SD)	458	0.460 (0.315–0.669)	<0.001
IDH status (Mut vs. WT)	525	0.495 (0.311–0.777)	0.003
Gender (Male vs. Female)	528	0.898 (0.637–1.266)	0.541
Race (White vs. Asian&Black or African American)	517	0.659 (0.303–1.383)	0.276
Age (>40 vs. ≤ 40)	528	1.164 (0.827–1.638)	0.384
Histological type (Oligoastrocytoma&Oligodendroglioma vs. Astrocytoma)	528	1.050 (0.737–1.496)	0.787
Laterality (Right vs. Left&Midline)	523	1.156 (0.821–1.631)	0.406

analysis of DLAT and tumor marker Ki67 in paraneoplastic and glioma tissues was then performed (Fig. 2B , 2C), which showed that DLAT and Ki67 were significant in gliomas compared to paraneoplastic tissues. Further, immunohistochemistry of common tumor markers in gliomas was also analyzed (Fig. 3).

3.2. Association of DLAT expression with clinicopathological variables

According to Table 1 and Fig. 4, overexpressed of DLAT was linked to WHO grade (G3 vs. G2, $p < 0.001$), IDH status (WT vs. MUT, $p < 0.001$), primary therapy outcome (PD&SD vs. PR&CR, $p < 0.001$), overall survival (OS) ($p < 0.001$), disease-specific survival (DSS) events ($p < 0.001$), and progression-free interval (PFI) events ($p < 0.05$).

As for the clinical and pathological distinctions among both the DLAT elevated and decreased expression groups, univariate logistic regression showed several, which include WHO grade (ratio [OR] = 2.040, 95 % CI = 1.413–2.957, $p < 0.001$), Primary therapy outcome (OR = 0.460, 95 % CI = 0.315–0.669, $p < 0.001$) and IDH status (OR = 0.495, 95 % CI = 0.311–0.777, $p = 0.003$) (Table 2).

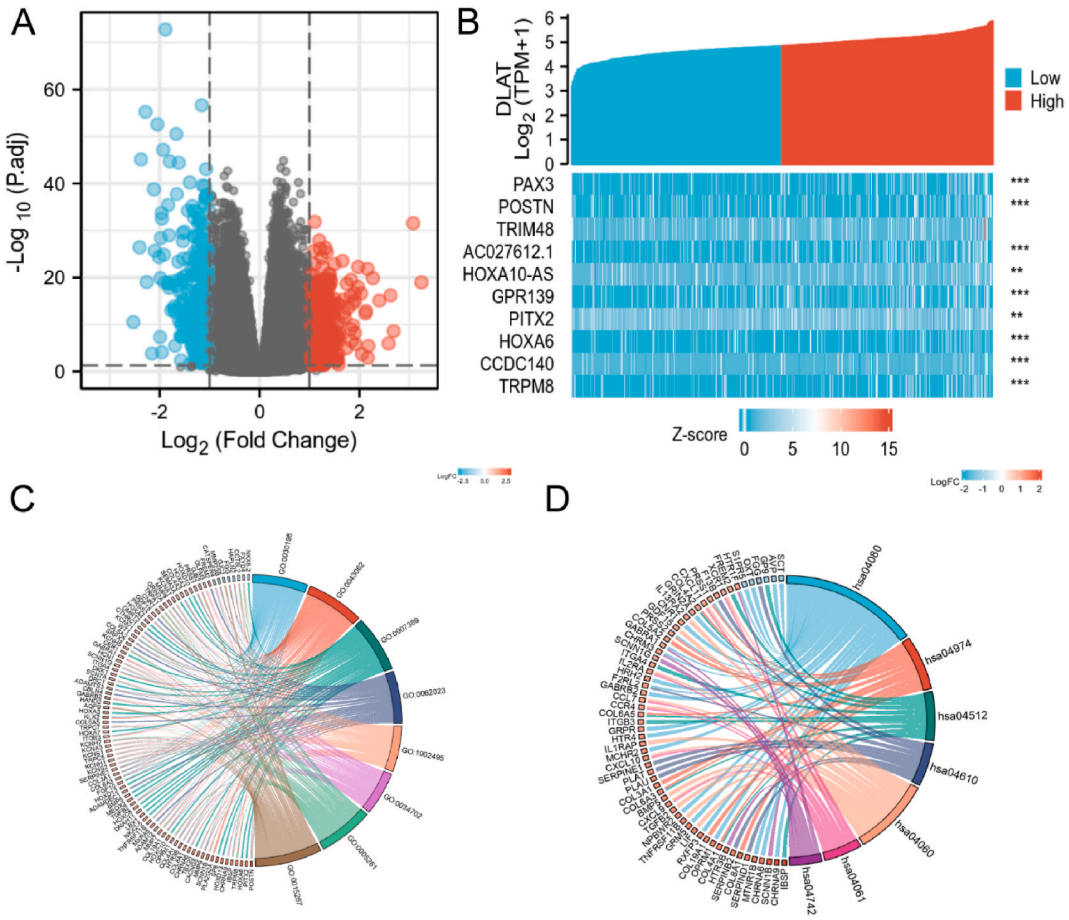

Fig. 5. DLAT-associated differentially expressed genes (DEG) and functional enrichment analysis of DLAT in low-grade gliomas using GO and KEGG. (A) Volcano plot. Blue and red dots indicate significantly down- and up-regulated DEGs, respectively. (B) Heat map of DLAT expression correlation with the top 10 DEGs. (C) GO enrichment analysis of DEGs. (D) KEGG enrichment analysis of DEGs. * $p < 0.05$, ** $p < 0.01$, *** $p < 0.001$.

3.3. Low-grade gliomas' DEG identification and functional enrichment evaluation

Fig. 5A and Supplementary Table 1 revealed that across the groups with both elevated and decreased DLAT expression, 818 genes met the criteria of |log2(FC)|>1 and p.adj <0.05, with 474 upregulated DEGs and 344 downregulated DEGs; then, the top ten genes (including PAX3, POSTN, TRIM48, AC027612.1 HOXA10-AS, GPR139, PITX2, HOXA6, CCDC140, TRPM8) were related to DLAT as shown in Fig. 5B. Further enrichment analysis of DEG was performed. Fig. 5C and Supplementary Table 2 revealed the extracellular matrix organization, transmembrane transporter complex, ion channel complex, and channel activity were among the GOs that DEG was enriched in, according to an examination of biological processes, cellular makeup, and molecular activities. Moreover, KEGG pathway research revealed that important approaches for DEGs enrichment encompassed neuroactive ligand-receptor interaction, protein digestion and absorption, ECM-receptor interaction, complement and coagulation cascades, etc (Fig. 5D and Supplementary Table 3). After this, GSEA comparison of the groups with both elevated and decreased DLAT expression revealed greater significant immune-related biological processes in decreased DLAT expression group, indicating that excessive DLAT level results in a diminished immune phenotype in low-grade gliomas (Fig. 6A–D).

3.4. Relation of methylation with DLAT level

We further looked at the relationship among both DLAT overexpression and methylation statuses through the use of a free tools to define the likely pathways of DLAT upregulation in cells of low-grade glioma. Fig. 7A demonstrates that the majority of methylation locations in DLAT Gene sequences remained hypermethylated for low-grade gliomas, and the level of methylation was linked with the prognosis of the patient (i.e., overall survival was lower in patients with low DLAT methylation levels than in sufferings with high DLAT methylation levels). Last but not least, a number of methylation sites—including cg16687867, cg17213552, and cg27191019—indicated a dismal outlook (Fig. 7B–D).

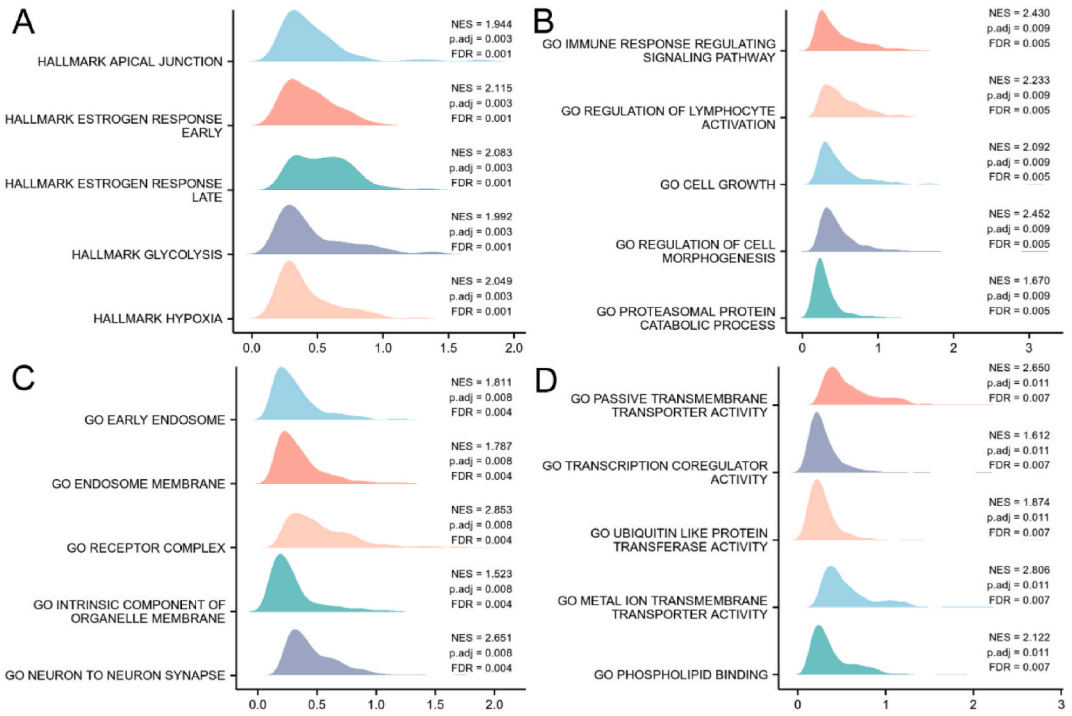

Fig. 6. Gene set enrichment analysis of DEG. (A) GSEA analysis of the Hall marker gene set deposited in MSigDB. (B) GSEA analysis of bp of gene sets downloaded from MSigDB. (C) GSEA analysis of cc of gene sets downloaded from MSigDB. (D) GSEA analysis of mf of the gene set of the gene book system downloaded from MSigDB.

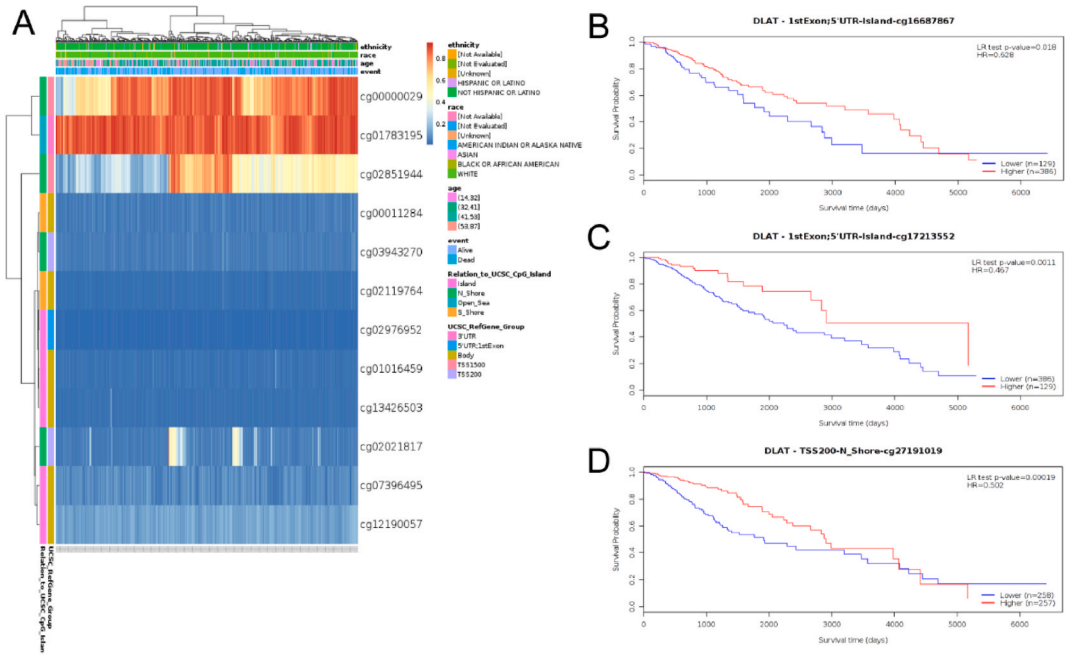

Fig. 7. DNA methylation level of DLAT and its impact on the prognosis of patients with low-grade glioma. (A) Correlation between DLAT mRNA expression levels and methylation levels. (B–D) Kaplan-Meier survival curves of several methylation sites of DLAT.

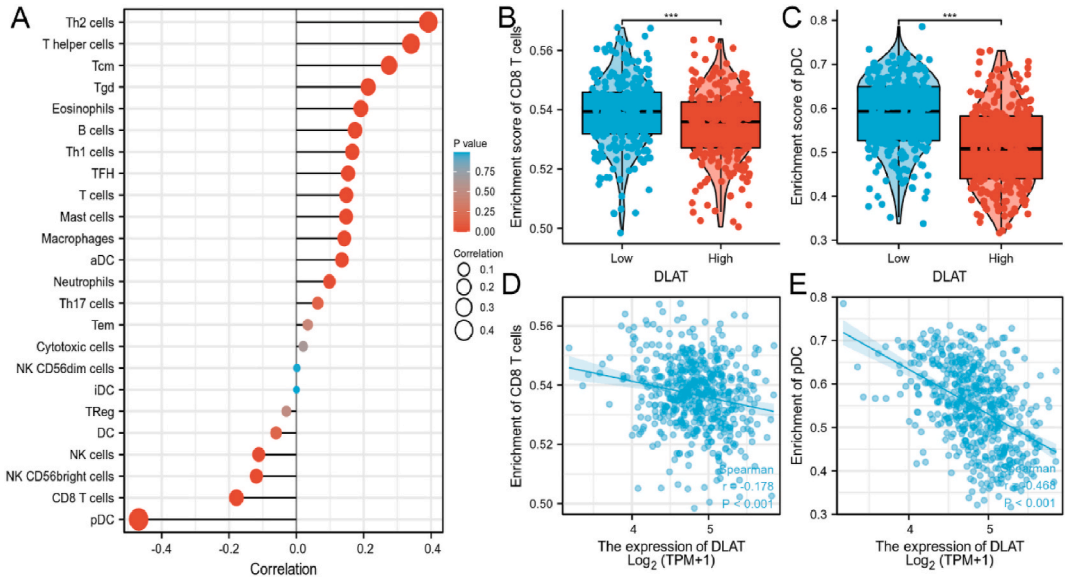

Fig. 8. Correlation of DLAT expression with the level of LGG immune infiltration. (A) Correlation of DLAT expression with the relative abundance of 24 immune cells. The size of the points corresponds to the absolute Spearman's correlation coefficient values. (B–C) Comparison of immune infiltration levels of immune cells (including pDC and $CD8^+$ T cells) in the DLAT high expression group and low expression group. (D–E) Correlation between the relative enrichment scores of immune cells (including pDC and $CD8^+$ T cells) and DLAT expression.

3.5. Relation of immune invasion and DLAT expression

In Fig. 8A, the degree of immunological cellular invasion by pDC ($r = -0.468$, $p < 0.001$) and CD8 T cells ($r = -0.178$, $p < 0.001$) was strongly adversely connected ($r = -0.210$, $p < 0.001$) with DLAT expression. Additionally, in Fig. 8B–E, pDC and CD8 T cell enrichment values were considerably reduced in the DLAT elevated expression team than in the DLAT decreased expression team (both <0.001).

3.6. Significance of DLAT for LGG patients' prognosis

The correlation across DLAT protein and the outlook of LGG sufferers was computed using the Kaplan-Meier technique. Sufferers were split into groups with elevated and decreased DLAT expression based on the median DLAT expression, which served as the threshold number. In comparison to the lower DLAT translation team, the prognosis for both OS and DSS was markedly worse in the higher DLAT translation team (OS: risk ratio [HR] = 1.49, 95 % CI = 1.05–2.12, p = 0.024; DSS: HR = 1.47, 95 % CI = 1.02–2.11, p = 0.04) (Fig. 9A and B).

As shown in Fig. 10, the prognosis of high DLAT expression in LGG patients with either OS or DSS had a poor prognosis in several subgroups, including (non-codel, Astrocytoma and Oligoastrocytoma, WT and MUT, age >40 years and Left and Right) (all $p < 0.05$), while the G2 and G3 subgroups had a poorer prognosis in OS only.

In Fig. 9C and Supplementary Table 4, to find prognostic markers, multivariate as well as univariate Cox regression tests seemed used. IDH status, the outcome of primary therapy (adjusted HR = 4.636, 95 % CI = 2.173–9.890, $p < 0.001$), and age (adjusted HR = 2.235, 95 % CI = 1.289–3.875, p = 0.004) were all independently associated with OS in LGG patients, according to the results of the multifactorial assessment. In the same way, Supplementary Figure 1 and Supplementary Table 5s demonstrated that IDH status, primary therapy outcome, and age were all predictors of DSS: adjusted HR = 2.301, 95 % CI = 1.304–4.061, p = 0.004, and IDH status, adjusted HR = 0.189, 95 % CI = 0.105–0.341, $p < 0.001$.

3.7. Nomogram graph construction and validation on the basis of variable independence

T Column line plots according to separate OS parameters in Fig. 11A were created to forecast the outcome of LGG sufferers. More total scores were linked to a worse prognosis on the column line graphs. Moreover, calibration curves were applied to evaluate how well the column line graphs predicted outcomes (Fig. 11B–D). The column line plot's bootstrap-corrected C index, which measures the model's prediction accuracy for OS in LGG patients, was 0.720 (95 % CI = 0.605–0.834). Moreover, ROC curves were employed to evaluate the DLAT expression's capacity for discrimination (Supplementary Figure 2). These results suggest that the column line plot is appropriate.

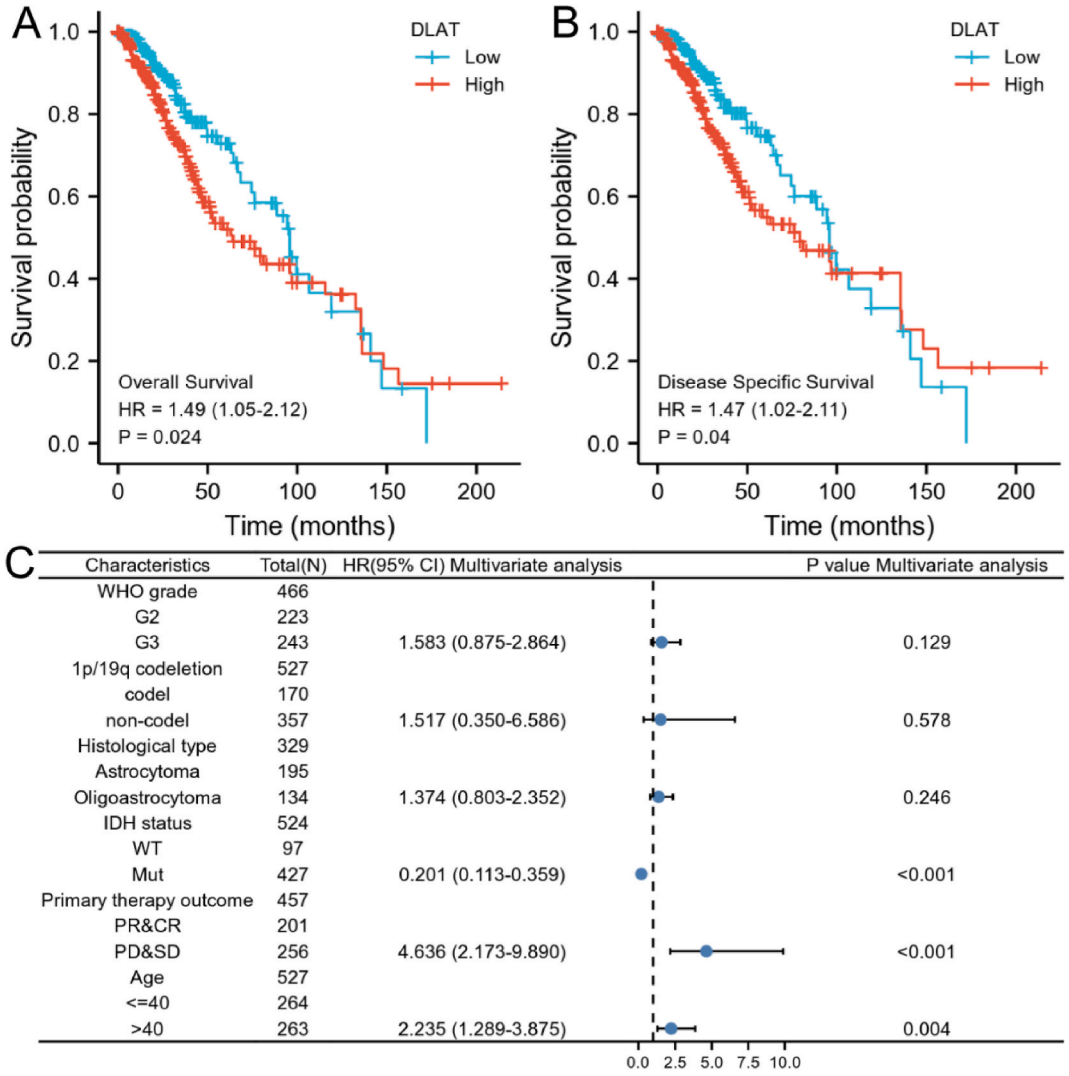

Fig. 9. Prognostic values of DLAT expression in LGG patients assessed by the Kaplan-Meier method. Overall survival (A) and disease-specific survival (B) of patients with high DLAT expression versus low DLAT expression in LGG. (C) Forest plot of overall survival based on multivariate Cox analysis.

4. Discussion

Among the most prevalent primary tumors, glioma can be clinically challenging to treat and frequently has a bad prognosis [33]. In contrast, low-grade gliomas account for approximately one-fifth of all gliomas, so we pay particular attention to the development of low-grade gliomas [34,35]. The microenvironment of LGG tumors has been found to be regulated by two cell types, immune cells and stromal cells. Finding more precise biomarkers to identify early carcinogenesis and track tumor progression using these two cell types is therefore crucial from a therapeutic standpoint [36,37].

Cuproptosis is a distinct form of apoptosis from oxidative stress-related apoptosis, in which the accumulation of lipid acylated proteins adversely impairs cells' ability to complete their TCA cycle and ultimately results in cell death [9]. The glycolytic molecule pyruvate, which is processed by the pyruvate dehydrogenase complex (PDC), can be oxidatively transformed to acetyl coenzyme A for the TCA cycle. While dihydrolipoyl transacetylase (DLAT) is an important component of PDC [38], therefore, DLAT may become a novel therapeutic target for LGG prognosis.

Although LGG is heterogeneous, existing pathology signals (such Ki67 and grading) for prognosis prediction contain drawbacks. Hence, finding new biomarkers is essential to improving tailored care and prognosis prediction. Within that research, the TCGA and GTEx databases were used to assess the DLAT expression in LGG. It was discovered that DLAT was overexpressed in LGG. Previous studies have confirmed that DLAT expression is also increased in several types of cancer, including cholangiocarcinoma [39], Colorectal Cancer [40], Stomach Cancer [17], and pancreatic cancer [41], in agreement with our pan-cancer studies' findings.

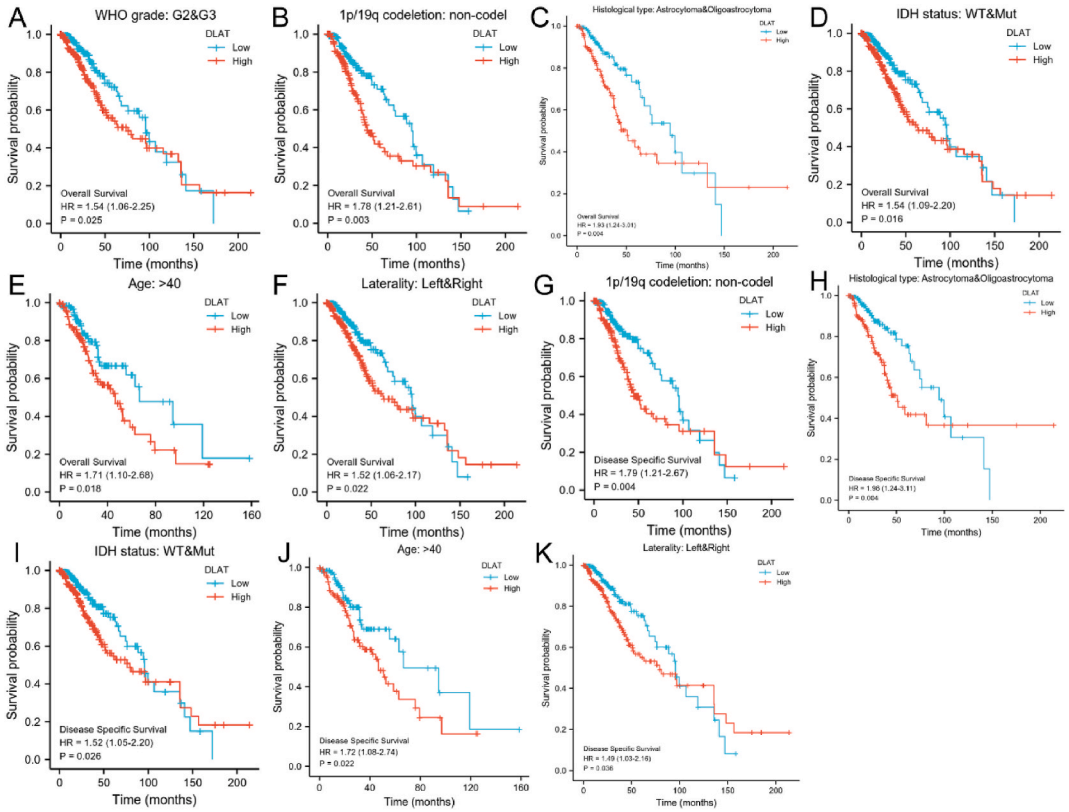

Fig. 10. Kaplan-Meier method to evaluate the prognostic value of DLAT expression in different subgroups of LGG patients. (A–F) OS survival curves of G2 and G3, non-codel, Astrocytoma and Oligoastrocytoma, WT and MUT, age >40 years and Left and Right subgroups between patients with high and low DLAT-expressing LGG. (G–K) DSS survival curves between high- and low-DLAT-expressing LGG patients with non-codel, Astrocytoma and Oligoastrocytoma, WT and MUT, age >40 years and Left and Right subgroups.

According to further investigation, elevated DLAT expression was linked to adverse clinicopathological traits like WHO grade, IDH status, primary therapy outcome, OS, DSS, and PFI. Furthermore, our analysis's findings indicate that DLAT overexpression is a distinct prognostic biomarker for bad OS and DSS in LGG sufferers. Previous research has indicated that the presence of DLAT may serve as a potential prognostic marker for a decreased prognosis in patients with a particular type of solid tumor, such as colorectal cancer [42], Pancreatic Cancer [43], Lung adenocarcinoma [12], Endometrial cancer [44]. These findings imply that DLAT may be a desirable new molecular target for potent cancer treatment.

The biological processes and signaling pathways of DLAT were further examined to investigate potential DLAT processes in LGG. GSEA enrichment analysis showed that pathways such as glycolysis, hypoxia, immune response-regulating signaling pathway, lymphocyte control, and neuron to neuron communication were mainly enriched in the group that had elevated DLAT transcription. The richness of DLAT-related biological processes in LGG may be enhanced by our findings, which still need more experimental validation.

A frequent epigenetic mechanism that often inhibits gene expression is DNA methylation [45]. The MethSurv database was utilized to explore the link among DLAT mRNA transcription and methylation levels, and the prognosis of DLAT methylation levels was examined. The outcomes suggested that DLAT overexpression and its DNA hypomethylation may be linked. And the poor prognosis of LGG patients was linked to the hypomethylation level of DLAT. It implies that DNA methylation may be crucial to the emergence of LGG.

The tumor cell microenvironment is generally regarded as having greater clinical significance for prognostic assessment of cancer identification because studies have shown that the majority of the expression of genes in tumor cells is affected by the cancerous cell microenvironment [35]. It has been shown that immune cells that infiltrate tumors have prognostic value, and this value depends on the type, density, and position of immune cells [46]. Infecting immune cells have also been demonstrated to forecast the effectiveness of immune checkpoint inhibition (ICI) therapy and neoadjuvant chemotherapy [47,48]. Gene expression profiling database and ssGSEA method of the R software package were used to investigate the association among both DLAT expression and immune cell infiltration. It was discovered that the degree of immunological cell infiltration of pDC and CD8 T cells had a strong negative link to DLAT expression. The enlargement values of pDC and CD8 T cells in the DLAT overexpression team were considerably lower than those in the decreased expression team, according to further analysis. Our findings imply that DLAT excessive expression could affect LGG prognosis and development by controlling the quantity of invading immune cells.

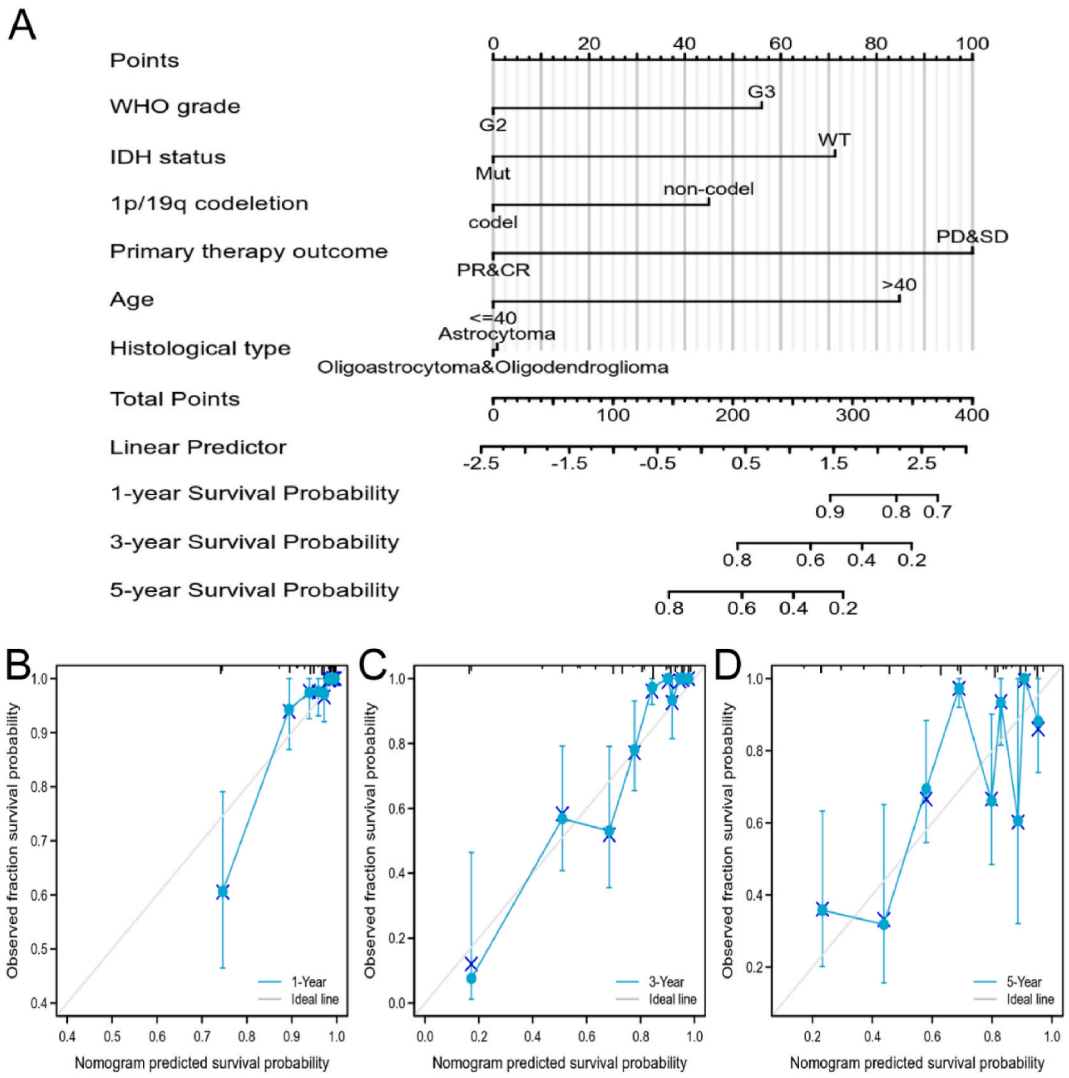

Fig. 11. Column plots and calibration curves predicting one-, three-, and five-year overall survival in patients with LGG. (A) Column line plots predicting one, three and five overall survival in LGG patients. (B–D) Calibration curves of predicted one-year, three-year and five-year overall survival nomograms for LGG patients.

There remain a few drawbacks to our current work, despite the fact that it sheds fresh light on the connection among both DLAT expression and the prognosis of sufferers with low-grade gliomas. First off, because all data utilized for the study's bioinformatics analyses were retrieved directly from public sources, we failed to collect key crucial medical evidence, like the patients' chemotherapy regimens; second, the sample size of the control group differed significantly from that of the tumor group, so much farther study relies on to an equitable split of large samples is required; third, To clarify the biochemical processes and possible procedures of DLAT in LGG, more research and rigorous experimental validation are needed for both in vitro as well as in vivo.

As a result, our article's findings indicate that severe clinical characteristics and adverse immune infiltration are strongly correlated with DLAT overexpression, which acts as an intrinsic bad predictive marker in LGG. The outcomes imply that DLAT may be employed as an innovative predictive biomarker to assess the prognosis of an individual. To confirm the process by which DLAT regulates LGG carcinogenesis and progression, more study is necessary.

5. Contributions

(I) Conception and design: H Cheng and X Dai; (II) Administrative support: X Dai (III); Provision of study materials or patients: P Gao and H Li (IV); Collection and assembly of data: Y Qiao, J Nie and S Cheng; (V) Data analysis and interpretation: G Tang, Y Qiao, H Li and P Gao; (VI) Manuscript writing: All authors; (VII) Final approval of manuscript: All authors.

Data availability

Data and download URLs involved in this study had been described in detail in the Methods section. All results generated in this study can be obtained by contacting the corresponding authors on reasonable request.

CRediT authorship contribution statement

Peng Gao: Writing – original draft, Validation. **Huaixu Li:** Writing – original draft, Validation, Resources, Investigation. **Yang Qiao:** Resources, Data curation. **Jianyu Nie:** Investigation, Formal analysis, Data curation. **Sheng Cheng:** Investigation, Data curation. **Guozhang Tang:** Investigation, Data curation. **Xingliang Dai:** Writing – review & editing, Project administration, Conceptualization. **Hongwei Cheng:** Writing – review & editing, Funding acquisition, Conceptualization.

Declaration of competing interest

The authors declare that they have no known competing financial interests or personal relationships that could have appeared to influence the work reported in this paper.

Acknowledgments

This study was supported by the Anhui Provincial Natural Science Foundation (2208085MH251), the Anhui Medical University Scientific Research Fund (No. 2021xkj131), the Basic and Clinical Cooperative Research and Promotion Program of Anhui Medical University (2021xkjT028), Health Research Program of Anhui (AHWJ2023A30007), Research Fund of Anhui Institute of Translational Medicine (2023zhyx-C19), and Anhui Provincial Department of Education Higher Education Quality Engineering Project (2022jyxm761).

Appendix A. Supplementary data

Supplementary data to this article can be found online at https://doi.org/10.1016/j.heliyon.2024.e32270.

References

[1] Y. Liu, et al., Photothermal therapy and photoacoustic imaging via nanotheranostics in fighting cancer, Chem. Soc. Rev. 48 (7) (2019) 2053–2108.
[2] H. Sung, et al., Global cancer statistics 2020: GLOBOCAN estimates of incidence and mortality worldwide for 36 cancers in 185 countries, CA Cancer J Clin 71 (3) (2021) 209–249.
[3] H. Qiu, et al., A prognostic microenvironment-related immune signature via ESTIMATE (PROMISE model) predicts overall survival of patients with glioma, Front. Oncol. 10 (2020) 580263.
[4] S. Solanki, et al., Inpatient burden of gastric cancer in the United States, Ann. Transl. Med. 7 (23) (2019) 772.
[5] D.N. Louis, et al., The 2021 WHO classification of tumors of the central nervous system: a summary, Neuro Oncol. 23 (8) (2021) 1231–1251.
[6] D. Kreatsoulas, et al., Supratotal surgical resection for low-grade glioma: a systematic review, Cancers 15 (9) (2023).
[7] B. Oldrini, et al., MGMT genomic rearrangements contribute to chemotherapy resistance in gliomas, Nat. Commun. 11 (1) (2020) 3883.
[8] H. Duffau, Oncological and functional neurosurgery: perspectives for the decade regarding diffuse gliomas, Rev. Neurol. (Paris) 179 (5) (2023) 437–448.
[9] P. Tsvetkov, et al., Copper induces cell death by targeting lipoylated TCA cycle proteins, Science 375 (6586) (2022) 1254–1261.
[10] X. Tang, et al., Copper in cancer: from limiting nutrient to therapeutic target, Front. Oncol. 13 (2023) 1209156.
[11] T. Wang, et al., Cuproptosis-related gene FDX1 expression correlates with the prognosis and tumor immune microenvironment in clear cell renal cell carcinoma, Front. Immunol. 13 (2022) 999823.
[12] S. Wang, et al., Comprehensive bioinformatics analysis to identify a novel cuproptosis-related prognostic signature and its ceRNA regulatory axis and candidate traditional Chinese medicine active ingredients in lung adenocarcinoma, Front. Pharmacol. 13 (2022) 971867.
[13] L. Deng, et al., Comprehensive analyses of PDHA1 that serves as a predictive biomarker for immunotherapy response in cancer, Front. Pharmacol. 13 (2022) 947372.
[14] R. Youssef, et al., Metabolic interplay in the tumor microenvironment: implications for immune function and anticancer response, Curr. Issues Mol. Biol. 45 (12) (2023) 9753–9767.
[15] R.B. Robey, et al., Metabolic reprogramming and dysregulated metabolism: cause, consequence and/or enabler of environmental carcinogenesis? Carcinogenesis 36 (Suppl 1) (2015) S203–S231.
[16] P.W. Stacpoole, Therapeutic targeting of the pyruvate dehydrogenase complex/pyruvate dehydrogenase kinase (PDC/PDK) Axis in cancer, J. Natl. Cancer Inst. 109 (11) (2017).
[17] W.Q. Goh, et al., DLAT subunit of the pyruvate dehydrogenase complex is upregulated in gastric cancer-implications in cancer therapy, Am J Transl Res 7 (6) (2015) 1140–1151.
[18] J. Vivian, et al., Toil enables reproducible, open source, big biomedical data analyses, Nat. Biotechnol. 35 (4) (2017) 314–316.
[19] L. Satgunaseelan, et al., Prognostic and predictive biomarkers in central nervous system tumours: the molecular state of play, Pathology 56 (2) (2023) 158–169.
[20] G. Khanna, et al., Immunohistochemical and molecular genetic study on epithelioid glioblastoma: series of seven cases with review of literature, Pathol. Res. Pract. 214 (5) (2018) 679–685.
[21] K.Z. Chen, et al., Vimentin as a potential target for diverse nervous system diseases, Neural Regen Res 18 (5) (2023) 969–975.
[22] K. Galbraith, M. Snuderl, Molecular pathology of gliomas, Surg Pathol Clin 14 (3) (2021) 379–386.
[23] X. Kong, et al., CD34 over-expression is associated with gliomas' higher WHO grade, Medicine (Baltim.) 95 (7) (2016) e2830.
[24] Y. Yang, et al., Identification of the immune landscapes and follicular helper T cell-related genes for the diagnosis of age-related macular degeneration, Diagnostics 13 (17) (2023).

[25] W. Walter, F. Sánchez-Cabo, M. Ricote, GOplot: an R package for visually combining expression data with functional analysis, Bioinformatics 31 (17) (2015) 2912–2914.
[26] X. Tu, et al., Single-cell transcriptomics reveals immune infiltrate in sepsis, Front. Pharmacol. 14 (2023) 1133145.
[27] D. Mitchell, S. Chintala, M. Dey, Plasmacytoid dendritic cell in immunity and cancer, J. Neuroimmunol. 322 (2018) 63–73.
[28] W.X. Huff, et al., The evolving role of CD8+CD28- immunosenescent T cells in cancer immunology, Int. J. Mol. Sci. 20 (11) (2019).
[29] G. Bindea, et al., Spatiotemporal dynamics of intratumoral immune cells reveal the immune landscape in human cancer, Immunity 39 (4) (2013) 782–795.
[30] V. Modhukur, et al., MethSurv: a web tool to perform multivariable survival analysis using DNA methylation data, Epigenomics 10 (3) (2018) 277–288.
[31] M.H. Nadimi-Shahraki, et al., Binary aquila optimizer for selecting effective features from medical data: a COVID-19 case study, Mathematics 10 (11) (2022).
[32] M. Singh, et al., Evolution of machine learning in tuberculosis diagnosis: a review of deep learning-based medical applications, Electronics 11 (17) (2022).
[33] F. Petralia, et al., Integrated proteogenomic characterization across major histological types of pediatric brain cancer, Cell 183 (7) (2020) 1962–1985.e31.
[34] N. Zhang, et al., FoxM1 promotes β-catenin nuclear localization and controls Wnt target-gene expression and glioma tumorigenesis, Cancer Cell 20 (4) (2011) 427–442.
[35] J.J. Wang, K.F. Lei, F. Han, Tumor microenvironment: recent advances in various cancer treatments, Eur. Rev. Med. Pharmacol. Sci. 22 (12) (2018) 3855–3864.
[36] T.F. Gajewski, H. Schreiber, Y.X. Fu, Innate and adaptive immune cells in the tumor microenvironment, Nat. Immunol. 14 (10) (2013) 1014–1022.
[37] A.E. Denton, E.W. Roberts, D.T. Fearon, Stromal cells in the tumor microenvironment, Adv. Exp. Med. Biol. 1060 (2018) 99–114.
[38] Q. Chen, et al., PM2.5 promotes NSCLC carcinogenesis through translationally and transcriptionally activating DLAT-mediated glycolysis reprograming, J. Exp. Clin. Cancer Res. 41 (1) (2022) 229.
[39] L. Wang, et al., Molecular cloning, and characterization and expression of dihydrolipoamide acetyltransferase component of murine pyruvate dehydrogenase complex in bile duct cancer cells, J. Gastroenterol. 37 (6) (2002) 449–454.
[40] S. Chen, et al., Mining novel cell glycolysis related gene markers that can predict the survival of colon adenocarcinoma patients, Biosci. Rep. 40 (8) (2020).
[41] X. Huang, et al., Cuproptosis-related gene index: a predictor for pancreatic cancer prognosis, immunotherapy efficacy, and chemosensitivity, Front. Immunol. 13 (2022) 978865.
[42] W. Wu, et al., Cuproptosis-Related genes in the prognosis of colorectal cancer and their correlation with the tumor microenvironment, Front. Genet. 13 (2022) 984158.
[43] Y. Xu, et al., Cuprotosis-related genes: predicting prognosis and immunotherapy sensitivity in pancreatic cancer patients, JAMA Oncol. 2022 (2022) 2363043.
[44] Y. Chen, Identification and validation of cuproptosis-related prognostic signature and associated regulatory Axis in uterine corpus endometrial carcinoma, Front. Genet. 13 (2022) 912037.
[45] K. Satomi, K. Ichimura, J. Shibahara, Decoding the DNA methylome of central nervous system tumors: an emerging modality for integrated diagnosis, Pathol. Int. 74 (2) (2024) 51–67.
[46] W. Widowati, et al., Effect of interleukins (IL-2, IL-15, IL-18) on receptors activation and cytotoxic activity of natural killer cells in breast cancer cell, Afr. Health Sci. 20 (2) (2020) 822–832.
[47] C. Denkert, et al., Tumor-associated lymphocytes as an independent predictor of response to neoadjuvant chemotherapy in breast cancer, J. Clin. Oncol. 28 (1) (2010) 105–113.
[48] J.J. Havel, D. Chowell, T.A. Chan, The evolving landscape of biomarkers for checkpoint inhibitor immunotherapy, Nat. Rev. Cancer 19 (3) (2019) 133–150.